SUPPLEMENTAL INFORMATION

Supplemental Figures

Supplemental Figure 1. Differentiating the fecal microbiota of CRON and AMER humans. (Related to Figure 1; Table S1; Table S2; Table S3) (A) PCoA plots of weighted UniFrac distances of lean AMER and CRON microbial communities. (**B)** Hierarchical clustering of the fecal microbiota of CRON and lean AMER subjects based on the proximity scores (1-proximity) from Random Forest classification. Bars represent the percentage of times that donor's fecal microbiota were correctly classified as either CRON or AMER in 100 independent runs of the algorithm. (**C)** A scatterplot shows the monotonically increasing relationship between feature importance scores (mean decrease in accuracy from the Random Forest classification averaged across 100 runs) for each OTU and its absolute difference in indicator values for the AMER and CRON DPs. (**D)** Linear correlation between *CIV* and *wCIV* across all human subjects.

Supplemental Figure 1

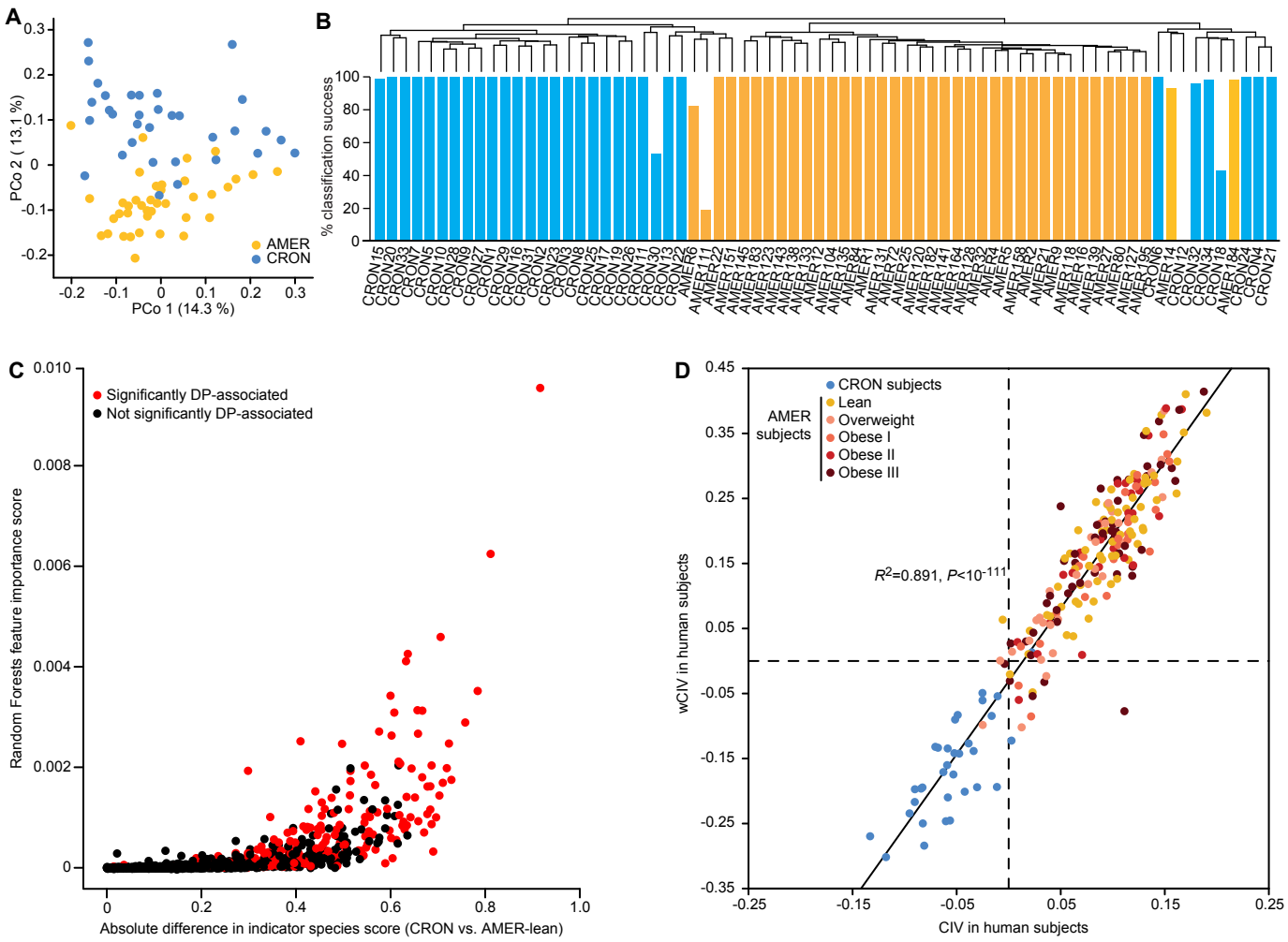

Supplemental Figure 2. Changes in phylogenetic diversity, the representation of DP-associated OTUs, and the representation of OTUs that differ in response to diet, throughout the different stages of the sequential cohousing experiment. (Related to Figure 4; Table S7; Table S8). Line graphs show each experimental mouse group's mean (±SEM) over time for **(A)** the aggregate percent abundance of AMER-associated OTUs, (**B**) the aggregate percent abundance of all CRON-associated OTUs, (**C**) phylogenetic diversity, **(D)** the number of CRON-associated OTUs detected, and **(E)** the number of AMER-associated OTUs in fecal samples collected from members of the different treatment groups. **(F)** Heatmap showing OTUs that differed significantly in their mean relative abundances on the tenth day of experimental Diet 1 versus the tenth day of Diet 2 (*n*=5 animals/treatment group). Significant differences, defined by Cochran-Mantel-Haenszel tests, are highlighted by cells with bold outlines. OTUs included in the heatmap had a mean percent abundance of ≥2.5% in at least one treatment group on experimental day 10 or 20 (end of Diet 1 or Diet 2, respectively), and differed by at least 1.0% in at least one group. AMER-associated taxa are highlighted in red text, while CRON-associated taxa are indicated by blue text. Hierarchical clustering of OTUs was based on the $\log_{10}$ of their mean abundances (per 10,000 reads) plus one pseudo-count.

Supplemental Figure 2

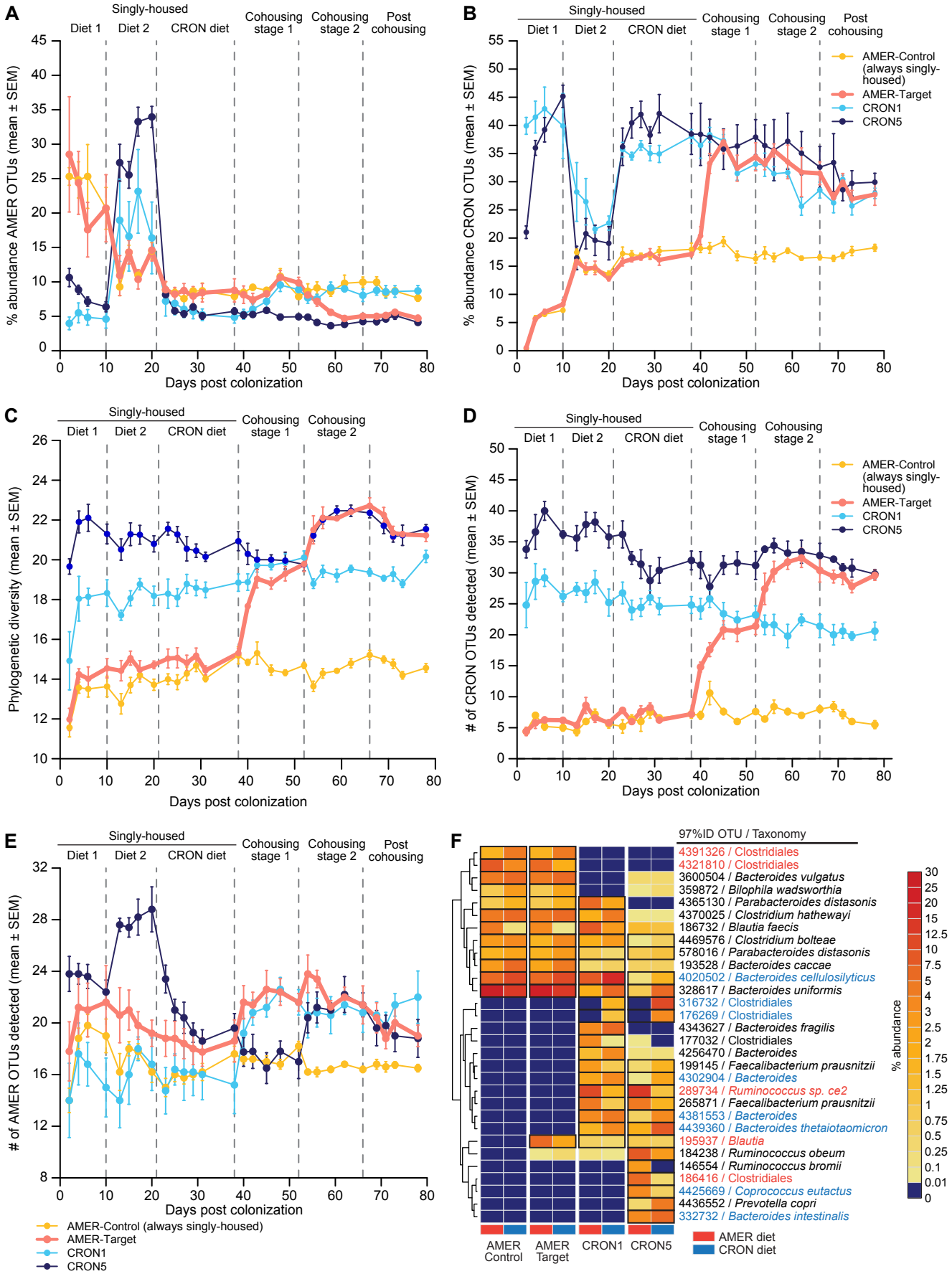

Supplemental Figure 3. Effects of diet switches and cohousing stages on community composition. (Related to Figure 4; Table S8). A phylogenetic tree shows 97%ID OTUs that initially established in the AMER-Target mouse microbiota or invaded during the two sequential cohousing stages. 97%ID OTUs in red represent established OTUs that had a mean relative abundance of at least 2 reads in 10,000 in the fecal microbiota of AMER-Target mice. OTUs in light blue indicate bacteria that successfully passed from CRON1 mice into AMER-Target mice during Cohousing stage 1, and OTUs in dark blue indicate OTUs that passed from CRON5 mice into AMER-Target mice during Cohousing stage 2. The tree was generated using the FastTree algorithm (Price et al., 2009).

Supplemental Figure 3

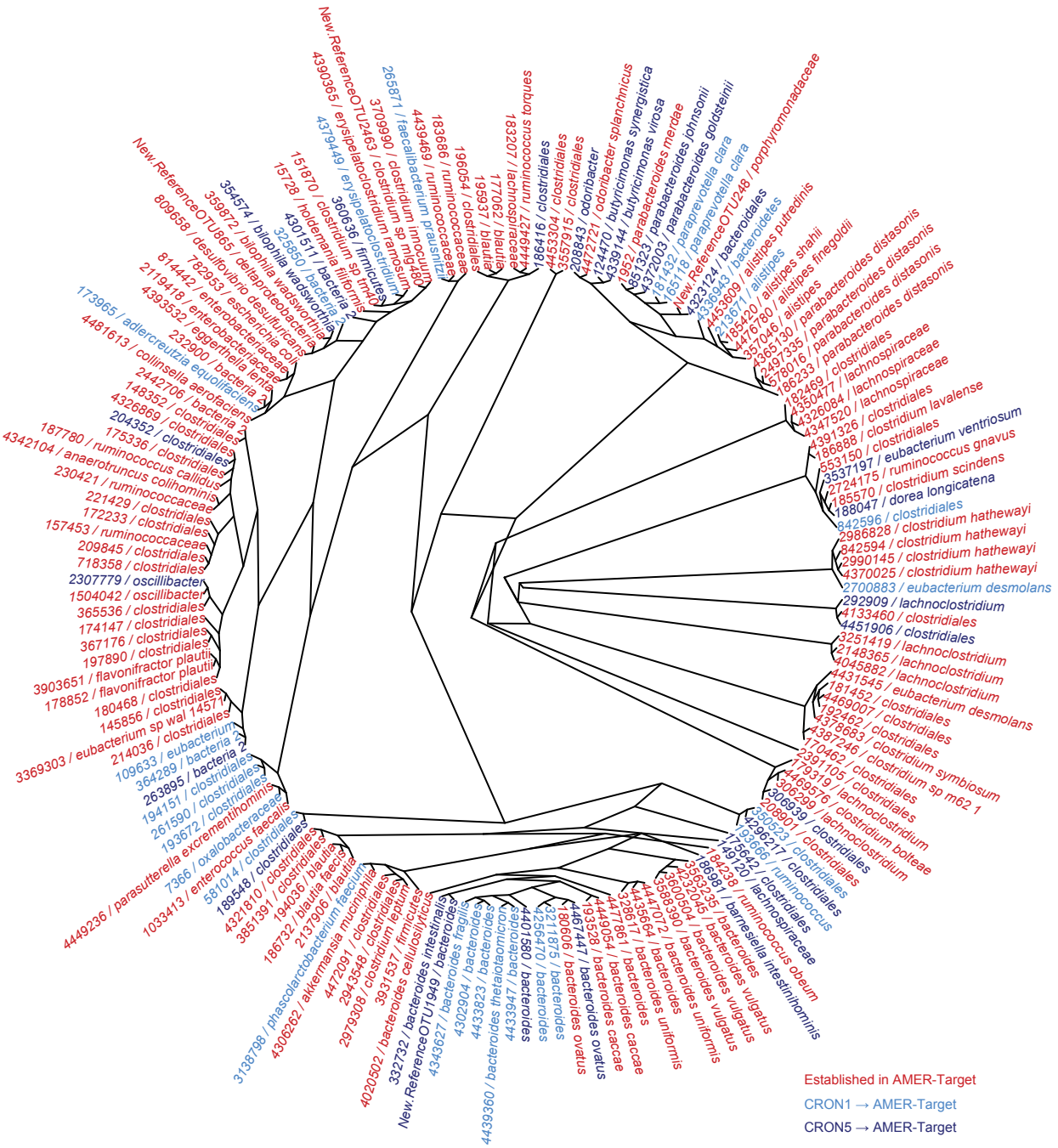

Supplemental Experimental Procedures

Diets

The two experimental diets were designed based on food journals kept by members of the Calorie Restriction Society and their non-restricted counterparts. For the CRON diet, 40 total days of consumption data were used (four days each from eight subjects and eight days from another), and 31 days' worth were used for the AMER diet (eight days each from three subjects and seven days from another). A dietician analyzed these journals with the Nutrition Data System for Research (NDS-R; version 4.03_31) to quantify the macronutrients and micronutrients consumed by each subject. The means of daily consumption of dietary energy (kilocalories), carbohydrates, proteins and fats were calculated for the CRON and AMER groups. These mean values served as the benchmarks against which *in silico* menus were evaluated. Randomly generated menus for each group were created by sampling 41 of the journal entries from all of the entries recorded by that group. One thousand randomized menus were generated. The representative diets manufactured were those with calculated values (based on the dietician's analyses of the journal entries' nutritional contents) with the closest values to the means presented in **Table S4A**. All *in silico* diet design procedures were conducted in software R v3.0.1 (R Core Team, 2016).

Ingredients were purchased at local grocery stores in St. Louis, Missouri, USA. Raw meats were cooked by boiling until well done. Eggs were hard-boiled. Ingredients were homogenized using a Robot Coupe R23 industrial food processor (Robot Coupe, Inc., Jackson, MI), and a Globe SP 30P mixer (Globe Food Equipment CO, Dayton, OH). Diets were then measured into ~500 g portions and placed into 3 mm thick vacuum-sealed bags (Uline, Inc., Pleasant Praire, WI; note that once this plastic bag was vacuum-sealed, it was placed in a second bag which was also vacuum-sealed). Diets were shipped overnight on ice for sterilization by gamma radiation (20 kGy-50 kGy; STERIS Corp, Mentor, OH). Nutritional analysis was then performed on the irradiated diets (NP Analytical Laboratories, St. Louis, MO).

Transplanting human fecal microbiota to gnotobiotic mice

For both the monotonous feeding experiment and the diet oscillation and cohousing experiment, C57BL/6J mice were maintained in plastic flexible film gnotobiotic isolators under a strict 12h light cycle (lights on at 0600). Transplantation of human fecal microbiota was performed as follows. Aliquots of frozen fecal samples from the human donors were resuspended by vortexing in 10 volumes (by weight) of filter-sterilized PBS supplemented with 0.05% L-cysteine-HCl and 0.1% resazurin in an anaerobic Coy chamber (Coy Lab Products, Grass Lake, MI) under an atmosphere of 75% N_2, 20% CO_2 and 5% H_2. The clarified samples were transferred to Balch tubes and carried in a secondary container to our gnotobiotic facility, where a single 200 μL aliquot was gavaged (via a syringe with a flexible sterile plastic tube) into the stomach of each mouse within its gnotobiotic isolator.

In the monotonous feeding experiment, germfree mice were initially fed an autoclaved low-fat, plant polysaccharide-rich diet (B&K Universal, East Yorkshire, U.K.) before being switched to the experimental diets at 11-12 weeks of age. During the subsequent two-week period, we monitored the average *ad libitum* consumption of the two diets in order to calibrate the amount used for experimental treatments. Mice were fed twice daily according to their diet treatments (AMER restricted, 4.0 g/day (provided and consumed); CRON restricted, 10 g/day (provided and consumed); mice feeding *ad libitum* were provided 10 g/day of the AMER diet or 20 g/day of the CRON diet). Animals were weighed in their gnotobiotic isolators weekly. Fresh fecal samples were collected throughout the experiment and temporarily stored at -20^{o}C before being moved to -80^{o}C until use. Mice were euthanized 63-64 days after gavage of donor microbiota. At sacrifice, total body weight and epididymal fat pad weights were recorded, and samples of cecal contents were immediately frozen at -80^{o}C for metabolite profiling. Procedures used for conducting the diet oscillation and cohousing experiment are described in detail in the main text and legend to **Figure 4**.

DNA isolation from human and mouse fecal samples and mouse cecal contents

Individual mouse fecal pellets or aliquots of mouse cecal contents or pulverized frozen human feces were placed in sterile 2.0 mL screw cap tubes with "O"-rings (Axygen Scientific, Union City, CA) containing a 3.97 mm steel ball and ~250 µL of 0.1 mm-diameter zirconia/silica beads. Eight hundred microliters of a 500:210 mixture of 20%SDS: 2X buffer A (200 mM NaCl, 200 mM Tris, 20 mM EDTA), plus 563 µL of a 25:24:1 mixture of phenol:chloroform:isoamyl alcohol were added. Samples were homogenized for 4 min using a Mini-Beadbeater-96 (Biospec Products, Inc., Bartlesville, OK) and then centrifuged at 3,220 x g for 7 min at room temperature. Four hundred eighty microliters of the aqueous phase from each sample were transferred to a 96-well plate. DNA was then isolated using QiaQuick 96 purification plates (Qiagen, Valencia, CA) as follows. Seven hundred twenty microliters of a 675:45 mixture of Qiagen buffer PM:3M sodium acetate (pH 5.5) was transferred to the QiaQuick 96 plate, stacked atop a Nunc 260251 plate (Thermo-Fisher Scientific, Rockford, IL). The aqueous phase was mixed by pipetting 180 µL up and down five times; 180 µL of the mixed aqueous phase was then transferred to the QiaQuick 96 plate and mixed with Quigen buffer PM:3M sodium acetate in the QiaQuick plate by pipetting 180 µL up and down 10 times. Plates were centrifuged for 15 min at 3,220 x g. Nine hundred microliters of Qiagen buffer PE were introduced and the plates were centrifuged for 4 min at 3,220 x g. This step was repeated for a second wash, except that centrifugation time was increased to 10 min. The QiaQuick 96 plates were subsequently dried in a speed-vac for 25 min; 100 µL of Qiagen buffer EB was added to each well and allowed to soak the membrane for 5 min. This step was followed by centrifugation for 2 min at 3,220 x g while stacked on 96-well plates to capture the eluates. DNA yield was measured with Quant-iT dsDNA Broad-Range Assay Kit (Invitrogen, Carlsbad, CA) and a Synergy 2 plate reader (BioTek Instruments, Inc., Winooski, VT) using Corning 3650 plates (Corning Life Sciences, Kennebunk, ME). All liquid-handling steps were performed using custom programs on a Genesis Series robot (Tecan Group, Ltd., Männedorf, CH) and a Biomek FX robot (Beckman Coulter, Brea, CA). A similar procedure was

used to isolate DNA from two samples of the representative irradiated CRON diet and three samples of the representative irradiated AMER diet (**Table S1D**).

Multiplex V4-16S rRNA amplicon sequencing

Protocols for PCR amplification of the V4 region of bacterial 16S rRNA genes present in each gut microbial community DNA sample, including descriptions of sample-specific barcoded primers and cycling conditions, methods for library preparation for sequencing with an Illumina MiSeq instrument, and processing of the resulting datasets are described by Bokulich et al. (2013). We trimmed the paired reads to 200 bases and assembled them using FLASH (v1.2.11) with default parameters, plus a minimum overlap of 18 bases and a maximum overlap of 125 bases (Magoč and Salzberg, 2011). Reads sharing at least 97% nucleotide sequence identity (97%ID) with a reference sequence in the GreenGenes 16S rRNA database (DeSantis et al., 2006) were assigned to that operational taxonomic unit (OTU). Unassigned sequences were subsequently grouped into *de novo* 97%ID OTUs. OTUs were assigned taxonomy using the RDP classifier (v2.4; Wang et al., 2007). A phylogenetic tree based on V4-16S rRNA sequences generated from this study was constructed and used to calculate metrics of phylogenetic diversity within and between samples. Before analysis, we removed 97%ID OTUs that failed sequence alignment by PyNast (Caporaso et al., 2010a). To be retained in the dataset OTUs had to satisfy at least one of the following conditions: (i) made up at least 0.05% of the reads in at least one human fecal sample, (ii) was detected in at least 1% of human donor fecal samples, (iii) made up at least 0.1% of the reads from at least one human, mouse fecal, or diet sample, or (v) was detected in at least 50% of the samples taken from at least one mouse. Samples with fewer than 10,000 reads, including two human samples were discarded before formal analyses.

Statistical analyses of 16S rRNA datasets

Sequencing data were rarefied to 10,000 reads per sample prior to analysis. Phylogenetic analysis, including calculation of UniFrac distances was performed in QIIME (v.1.5.0-dev; Caporaso et al., 2010b). ANOVA and mixed-effects ANOVA analyses were performed in R

v.3.2.2 (R Core Team, 2016), using the "lmerTest" (Kuznetsova et al., 2016), "lme4 " (Bates et al., 2015), and "lsmeans" (Lenth, 2016) packages. Mixed-effects analyses used the individual donors and mice as random effects where appropriate. Principal coordinates analysis was performed with the "ape" package (Paradis et al., 2004). PERMANOVA was performed with the "vegan" package (Oksanen et al., 2016). Indicator species analyses were performed using the "indicspecies" package (De Cáceres and Legendre, 2009). Prior to indicator species analysis, OTUs not present in the fecal microbiota of at least 20% of CRON or 20% of AMER individuals and having a mean percent abundance, when present, of at least 0.05% were removed to limit the number of necessary tests. For both indicator species analysis and phi-coefficient analysis, 10,000 permutations were used in significance tests. Supervised learning with Random Forest classifiers was also performed in R, using the "randomForest" package (Liaw and Wiener, 2002); 100 separate implementations were performed, and the mean proximities and feature importance scores were recorded and used in further analyses. Hierarchical clustering was performed on Bray-Curtis dissimilarities calculated from Wisconsin square-root transformed abundance data.

OTUs that successfully invaded members of each group of mice during cohousing were identified by a multi-step phi-coefficient analysis. A separate analysis was performed for each cohousing stage and invasion direction (i.e., CRON→AMER, AMER→CRON). OTUs retained in the analysis were (i) detected in the human subjects, (ii) present in at least three mice in at least one of the groups to be cohoused, and (iii) had a mean percent abundance of ≥0.05% (when present) in at least one of these groups. For each cohousing stage, OTUs were identified as invaders in the AMER→CRON direction if they were (i) significantly associated (P_{FDR}<0.05) with the AMER-Target mice in a phi-coefficient test of samples taken before the cohousing stage, (ii) present in at least two of the CRON-colonized mice at a mean percent abundance of 0.05% during the cohousing stage, and (iii) significantly associated with samples taken from the CRON-colonized mice during cohousing stage (P_{FDR}<0.05; phi-coefficient ≥0.6) in a phi-coefficient comparison against those samples taken pre-cohousing. OTUs were identified as invaders in the

CRON→AMER direction if they were (i) significantly associated (P_{FDR}<0.05) with the CRON1 or CRON5 animals (Cohousing stages 1 and 2, respectively) in a phi-coefficient test of samples taken before the cohousing stage, (ii) present in at least two of the AMER-Target mice at a mean percent abundance of 0.05% during the cohousing stage, (iii) significantly associated with samples taken from the AMER-Target mice during the cohousing stage (P_{FDR}<0.05; phi-coefficient ≥0.6) in a phi-coefficient comparison against those fecal samples taken pre-cohousing, and (iv) significantly associated (P_{FDR}<0.05) with the AMER-Target mice compared to the AMER-Control mice in samples taken during the cohousing stage.

GC-MS analysis of cecal metabolites

Non-targeted - Cecal contents were homogenized in 20 vol/wt of HPLC grade water and centrifuged (20,800 x g for 10 min at 4°C). A 200-µL aliquot of the resulting supernatant was transferred to a clean 2 mL glass tube (Agilent) and combined with ice-cold methanol (400 µL). The mixture was vortexed and centrifuged (20,800 x g for 10 min at 4°C). A 500-µL aliquot of the supernatant was mixed with 10 µL of lysine-$^{13}C_6$,$^{15}N_2$ (2 mM), and the mixture was evaporated to dryness using a speed vacuum. Samples were then treated with 80 µL of methoxylamine (15 mg/mL in pyridine) and incubated for 16 h at 37°C, followed by addition of 80 µL of *N*-methyl-*N*-(trimethylsilyl) trifluoroacetamide (containing a 1% v/v catalytic admixture of trimethylchlorosilane) and incubation for 1h at 70ºC (to derivatize methoximate reactive carbonyls and replace exchangeable protons with trimethylsilyl groups). Heptane (160 µL) was added before injecting 1-µL aliquots of each derivatized sample into an Agilent Model 5975C GC-MS system. Metabolites were identified by co-characterization of standards.

Targeted – Methods for UPLC-MS analysis of bile acids and GC-MS analysis of short-chain fatty acids are described in our previous publications (Dey et al., 2015; Wu et al., 2015).

MS-MS analysis of liver metabolites

Liver samples stored at -80°C were weighed and homogenized by bead beating in a solution of 50% aqueous acetonitrile and 0.3% formic acid (50 mg tissue per ml solution). Amino acids and acylcarnitines were measured using a Waters Acquity UPLC system with a triple quadrupole detector and the MassLynx 4.1 operating system (Waters, Milford, MA) (An et al., 2004; Ferrara et al., 2008). Previously published methods were used for extracting and purifying acyl-CoAs (Monetti et al., 2007). Acyl-CoAs were measured by flow injection with positive electroscopy ionization on a Xevo TQ-S mass spectrometer (Waters), using heptadecanoyl-CoA as an internal standard. Ceramides were extracted according to previously published protocols (Merrill et al., 2005) and also analyzed with the Xevo TQ-S mass spectrometer. Organic acids were measured with a Trace Ultra GC coupled to an ISQ MS with Xcalibur 2.2 (Thermo Fisher Scientific, Austin, TX) (Jensen et al., 2006).

Supplemental References

An, J., Muoio, D.M., Shiota, M., Fujimoto, Y., Cline, G.W., Shulman, G.I., Koves, T.R., Stevens, R., Millington, D., and Newgard, C.B. (2004). Hepatic expression of malonyl-CoA decarboxylase reverses muscle, liver and whole-animal insulin resistance. Nat. Med. *10*, 268-274.

Bates, D., Maechler, M., Bolker, B., and Walker, S. (2015). Fitting linear mixed-effects models using lme4. J. Statistical Software *67*, 1-48.

Bokulich, N.A., Ohta, M., Richardson, P.M., and Mills, D.A. (2013). Monitoring seasonal changes in winery-resident microbiota. PLoS ONE *8*, e66437.

Caporaso, J.G., Bittinger, K., Bushman, F.D., DeSantis, T.Z., Andersen, G.L., and Knight, R. (2010a). PyNAST: a flexible tool for aligning sequences to a template alignment. Bioinformatics *26*, 266-267.

Caporaso, J.G., Kuczynski, J., Stombaugh, J., Bittinger, K., Bushman, F.D., Costello, E.K., Fierer, N., Pena, A.G., Goodrich, J.K., Gordon, J.I., et al. (2010b). QIIME allows analysis of high-throughput community sequencing data. Nat. Methods *7*, 335-336.

De Cáceres, M., and Legendre, P. (2009). Associations between species and groups of sites: indices and statistical inference. Ecology *90*, 3566-3574.

DeSantis, T.Z., Hugenholtz, P., Larsen, N., Rojas, M., Brodie, E.L., Keller, K., Huber, T., Dalevi, D., Hu, P., and Anderson, G.L. (2006). Greengenes, a chimera-checked 16S rRNA gene database and workbench compatible with ARB. Appl. Environ. Microbiol. *72*, 5069-5072.

Dey, N., Wagner, V.E., Blanton, L.V., Cheng, J., Fontana, L., Haque, R., Ahmed, T., and Gordon, J.I. (2015). Regulators of gut motility revealed by a gnotobiotic model o diet-microbiome interaction related to travel. Cell *163*, 95-107

Ferrara, C.T., Wang, P., Neto, E.C., Stevens, R.D., Bain, J.R., Wenner, B.R., Ilkayeva, O.R., Keller, M.P., Blasiole, D.A., Kendziorski, C., et al. (2008). Genetic networks of liver metabolism revealed by integration of metabolic and transcriptional profiling. PLoS Genet. *4*, e1000034.

Jensen, M.V., Joseph, J.W., Ilkayeva, O., Burgess, S., Lu, D., Ronnebaum, S.M., Odegaard, M., Becker, T.C., Sherry, A.D., and Newgard, C.B. (2006). Compensatory responses to pyruvate carboxylase suppression in islet beta-cells. Preservation of glucose-stimulated insulin secretion. J. Biol. Chem. *281*, 22342-22351.

Kuznetzova, A., Brockhoff, P.B., and Christensen, R.H.B. (2016). lmerTest: tests in linear mixed effects models. https://CRAN.R-project.org/package=lmerTest.

Lenth, R.V. (2016). Least-squares means: the R package lsmeans. J. Statistical Software *69*, 1-33.

Liaw, A., and Wiener, M. (2002). Classification and regression by randomForest. R News *2*, 18-22.

Magoč, T., and Salzberg, S.L. (2011). FLASH: fast length adjustment of short reads to improve genome assemblies. Bioinformatics *27*:2957-2963.

Merrill, A.H., Sullards, M.C., Allegood, J.C., Kelly, S., and Wang, E. (2005). Sphigolipidomics: high-throughput, structure-specific, and quantitative analysis of sphingolipids by liquid chromatography tandem mass spectrometry. Methods *36*, 207-224.

Monetti, M., Levin, M.C., Watt, M.J., Sajan, M.P., Marmor, S., Hubbard, B.K., Stevens, R.D., Bain, J.R., Newgard, C.B., Farese, R.V. Sr., et al. (2007). Dissociation of hepatic steatosis and insulin resistance in mice overexpressing DGAT in the liver. Cell Metab. *6*, 69-78.

Oksanen, J., Blanchet, F.G., Kindt, R., Legendre, P., Minchin, P.R., O'Hara, R.B., Simpson, G.L., Solymos, P., Stevens, M.H.H., and Wagner, H. (2016). vegan: community ecology package. https://CRAN.R-project.org/package=vegan.

Paradis, E., Claude, J., and Strimmer, K. (2004). APE: analyses of phylogenetics and evolution in R language. Bioinformatics *20*, 289-290.

Price, M.N., Dehal, P.S., and Arkin, A.P. (2009). FastTree: Computing large minimum evolution trees with profiles instead of a distance matrix. Mol. Biol. Evol. *26*, 1641-1650.

R Core Team. (2016). R: a language and environment for statistical computing. URL https://www.R-project.org/.

Wang, Q., Garrity, G.M., Tiedje, J.M., and Cole, J.R. (2007). Naïve bayesian classifier for rapid assignment of rRNA sequences into the new bacterial taxonomy. Appl. Environ. Microbiol. *73*, 5261-5267.

Wu, M., McNulty, N.P., Rodionov, D.A., Khoroshkin, M.S., Griffin, N.W., Cheng, J., Latreille, P., Kerstetter, R.A., Terrapon, N., Henrissat, B., et al. (2015). Genetic determinants of in vivo fitness and diet responsiveness in multiple human gut *Bacteroides*. Science *350*, aac5992.

Supplemental Tables

Table S1. Human fecal, mouse fecal and cecal, and diet samples used for bacterial 16S rRNA amplicon sequencing and associated subject data and experimental treatments. (Related to Figure 1; Figure 2; Figure 4; Figure S1)

Table S2. Analyses of alpha-diversity and beta-diversity in CRON and AMER human subjects. (Related to Figure 1; Figure S1)

Table S3. DP-associated OTUs in CRON and AMER subjects. (Related to Figure 1; Figure S1)

Table S4. Summaries of the diets of CRON and AMER subjects, and recipes for representative CRON and AMER diets. (Related to Figure 2; Figure 4)

Table S5. Analyses of the fecal microbiota and morphometrics of AMER-colonized and CRON-colonized mice monotonously fed the AMER or CRON diet. (Related to Figure 2; Figure 3)

Table S6. Alpha-diversity and dietary practice-associated OTUs in the fecal microbiota of mice with different histories of exposure to CRON donor microbiota. (Related to Figure 4; Figure S2)

Table S7. OTUs that differed in relative abundance during pre-cohousing diet oscillations and OTUs that successfully migrated between mice during cohousing. (Related to Figure 4; Figure S2; Figure S3).

Table S8. Metabolite profiles in cecal contents and liver samples from mice with different histories of exposure to CRON donor microbiota. (Related to Figure 4; Figure 5)